Evaluation of Relationships between Precipitation, Temperature in Fukuoka and Climate Patterns

Iseri, Y.[1], D. Satomura[2], K. Jinno[1] and A. Kawamura[3]

[1]Department of Urban and Environmental Engineering, Kyushu University, Japan
Institute of Environmental Systems, Kyushu University, Japan
[2]Ministry of Land, Infrastructure and Transport, Kinki Regional Development Bureau, Japan
[3]Department of Civil and Environmental Engineering, Tokyo Metropolitan University, Japan
Email: hyd11@civil.kyushu-u.ac.jp

Keywords: *climate pattern, climate indices, Self-Organizing Maps, classification, Fukuoka city, rainfall, temperature*

EXTENDED ABSTRACT

A number of studies have discussed connections between El Niño phenomenon and unusual weather. Although El Niño phenomenon has obvious impacts on weather of the low-latitude area surrounding the Pacific, the connections between El ñino and unusual weather in mid-latitude area are not fully understood. The distance between mid-latitude and the area where the El Niño happens would be crucial reason why their relationships are rather obscure. Moreover, the weather in mid-latitude is not only affected by El Niño but also by several other kinds of climate factors such as intensity of Aleutian low pressure system. These complexities also obscure the influence of El Niño on the weather in mid-latitude and impose the need of considering several kinds of climate phenomena simultaneously in order to understand the unusual weather in mid-latitude.

This study has two objectives. The first objective is to classify climate patterns in the past using non-linear classification method, which is Self-Organizing Maps. The Self-Organizing Maps (SOM) algorithm is utilized as a classification method, because the SOM is capable of classifying high dimensional data on low dimensional arrays, enabling us to recognize hidden patterns in high dimensional data. The second objective of this study is to investigate the possible relationships between the classified climate patterns and rainfall and temperature in the city of Fukuoka, Japan.

In order to classify climate patterns, we use several kinds of climate indicators, namely the Southern Oscillation Index (SOI), Pacific Decadal Oscillation Index (PDOI), North Pacific Index (NPI), and Dipole Mode Index (DMI) for the period 1901 to 2002. The application of SOM for these indices detects climate patterns which occurred during the first two decades of the twentieth century and also detects the patterns which have been observed since the 1960s.

Investigation of the relationships between the identified climate pattern and rainfall and temperature in Fukuoka reveals that when La Niña phenomenon happens, PDO is in strong negative phase, the development of Aleutian low is weak and dipole mode in the Indian Ocean is in strong negative mode, AMJ (April, May and June) and JAS (July, August and September) temperature of Fukuoka in the next year tend to become extremely low.

1. INTRODUCTION

A number of studies have investigated the impacts of climate change on weather in various locations over the world (Beniston *et al*, 1994; Qian *et al*, 2001). One of the most prominent climate phenomena is ENSO (El Niño Southern Oscillation), of which extensive studies have been done in order to reveal the mechanism of its occurrence and to investigate relationships between the occurrence of El Niño (or La Niña) and unusual weather in various places (Rolelewski and Halpert, 1987). Although the impacts of El Niño on regional weather is reasonably clear in the low latitudes surrounding the Pacific, the impacts on mid latitudes is rather obscure. One of the principal reasons for this difficulty in mid latitudes would be the distance from the tropical zone where ENSO event occurs. The facts that weather in mid latitudes is not only affected by ENSO but also by various kinds of atmospheric-oceanic factors, such as the development of Aleutian low, would be also crucial reasons why impacts of El Niño for mid latitudes have indistinctness. For these reasons, if we considered the state of various climate factors simultaneously, it would be very helpful in evaluating the relationships between climate factors and their impacts on mid latitudes.

One of the objectives of this study is to identify climate patterns represented by four different kinds of atmospheric-oceanic indices: SOI (Southern Oscillation Index), PDOI (Pacific Decadal Oscillation Index), NPI (North Pacific Index) and DMI (Dipole Mode Index) for the period 1901 to 2002. We employ Self-Organizing Maps (SOM) in order to classify climate patterns that appeared during the period from 1901 to 2002. Another objective of this study is to investigate the possible relationships between the classified climate patterns and rainfall and temperature in the city of Fukuoka, Japan.

2. DATA

The Southern Oscillation Index (SOI), Pacific Decadal Oscillation Index (PDOI), North Pacific Index (NPI) and Dipole Mode Index (DMI) are used to investigate the relationship between large scale climate factors and the precipitation and temperature in the city of Fukuoka. The original data are at the monthly scale. However, we compute annual averaged time series for each of the climate indices, and then transform each of the annual averaged time series into the non-exceedance probability time series. The non-exceedance probability time series are used for the analysis in this study. The data period used in the analysis is from 1901 to 2002.

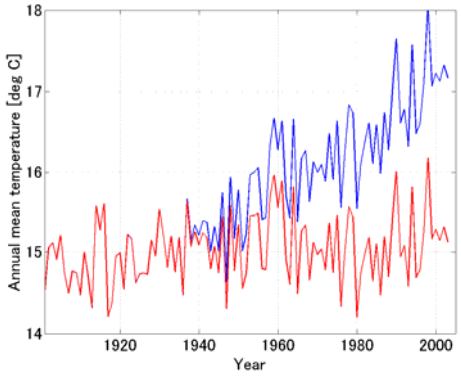

Figure 1. annual mean temperature (blue line) and detrended annual mean temperature (red line) in Fukuoka. Horizontal axis shows year and vertical axis shows temperatures in degree C.

2.1. Precipitation and temperature in Fukuoka

Precipitation and temperature in Fukuoka have been recorded since January 1890. As the temperature in Fukuoka has remarkably increasing trend, we estimate the linear trend after the year of 1937 against annual mean temperature using least square method, and remove the estimated linear trend from the original time series (Figure 1). The detrended temperature is used throughout this study.

2.2. SOI

A well-known atmospheric phenomenon is the Southern Oscillation (SO). The SO is an atmospheric see-saw process in the tropical Pacific sea level pressure between the eastern and western hemispheres associated with the El Niño and La Niña oceanographic features. The oscillation can be characterized by a simple index, the Southern Oscillation Index (SOI). (Kawamura *et al.* 1998). This index is used by NOAA (The National Oceanic and Atmospheric Administration) to evaluate when El Niño and La Niña occur (*Japanese Study Group for Climate Impact & Application* 1999). The feature is known as the El Niño Southern Oscillation (ENSO) phenomenon. The SOI is derived from monthly mean sea level pressure differences between Papeete, Tahiti (149.6°W, 17.5°S) and Darwin, Australia (130.9°E, 12.4°S). The database for the calculation of the SOI in the present study consists of 137 years of monthly mean sea level pressure data at Tahiti and Darwin from January 1866 to December 2002. The data are from Ropelewski and Jones (1987) and Allan *et al.* (1991), who carefully infilled all missing values by correlation with data from other observation stations. The data before 1920 are somewhat less reliable than the latter ones (Kawamura *et al.* 1998). For details of statistical

and long-term characteristics of SO, SOI and their barometric pressure data, refer to Kawamura *et al.* (2002) and Jin *et al.* (2003).

2.2. PDOI

The Pacific Decadal Oscillation (PDO) is described as a long-lived pattern of Pacific climate variability, somewhat like El Niño. PDO has two phases (the warm and cool phases), and each phase persisted for 20 to 30 years in the 20th century. The fingerprints of PDO are most visible in the North Pacific/North American region. Several studies found evidence for just two full PDO cycles in the past century: cool phases occurred during the periods 1890-1924 and 1947-1976, while warm phases prevailed during the periods of 1925-1946 and 1977 through the mid-1990s (Mantua *et al*. 1997).

PDOI is the leading principal component of monthly sea surface temperature (SST) anomalies in the North Pacific Ocean north of 20°N (Zhang *et al.* 1997; Mantua *et al.* 1997). The PDOI data since 1900, which are used in this study, are from the website of the Joint Institute for the Study of the Atmosphere and Ocean [http://tao.atmos. washington.edu/main.html].

2.3. NPI

Trenberth and Hurrell (1994) have defined the North Pacific Index (NPI) as the area-weighted sea level pressure over the region 30°N to 65°N, 160°E to 140°W to measure the decadal variations of atmosphere and ocean in the north Pacific. They found that this index is highly correlated with the leading principal component of the 500 hPa geopotential height. NPI is also a good index for the intensity of the Aleutian Low pressure cell. NPI data since 1899 are from the website of the University Corporation for Atmospheric Research [http://www.ucar. edu/ucar/index.html].

2.4. DMI

Saji *et al* (1999) have reported a dipole mode in the Indian Ocean, a pattern of internal variability with anomalously low sea surface temperatures off Sumatra and high sea surface temperatures in the western Indian Ocean, with accompanying wind and precipitation anomalies. The intensity of the dipole mode can be defined using the Dipole Mode Index, which describes the difference in the sea surface temperature anomaly between the tropical Indian Ocean (50°E-70°E, 10°S-10°N) and the tropical south-eastern Indian Ocean (90°E-110°E, 10°S-Equator).

3. METHODS

3.1. Self-Organizing Maps

In this study, the Self-Organizing Maps (SOM) algorithm is employed in order to classify the climate patterns represented by the above four kinds of climate indices, because the SOM is capable of classifying high-dimensional data on low-dimensional arrays, enabling us to compare patterns in high-dimensional data (e.g. climate patterns represented by the four kinds of climate indices).

The Self-Organizing Map (SOM) is an unsupervised learning algorithm, which was proposed by T. Kohonen (1992). The SOM has its advantages in visualization and abstraction of complex nonlinear statistical relationships in a set of data. The SOM enables the visualization and abstraction by compressing the information in high-dimensional data onto low-dimensional regular grids.

The following explains a basic version of the SOM algorithm, although many versions of the SOM exist. Suppose we have s samples and each of the samples consists of d dimensions. Each of the samples is denoted as input vector x, and thus every input vector has d dimension. The application of SOM on a given data set creates two-dimensional map that is composed of a number of nodes. Every node i on the map contains a reference vector r_i, which has d dimensions.

The following procedures describe how reference vectors learn the representative patterns in input vectors. The first step is to detect winner node m_w. A randomly selected input vector x is compared with every reference vectors. Although this comparison can be done using any metric, Euclid distance is usually used. By comparing the distance between the input vector x and every r_i using the metric, the winner node m_w is identified.

The second step updates reference vector in the node i. After the identification of winner node m_w, the following equation updates the reference vector r_i:

$$r_i(t+1) = r_i(t) + h_{wi}(t)\left[x(t) - r_i(t)\right] \quad (1)$$

where t refers to the regression step, and $h_{wi}(t)$ is a neighborhood function. In this study, the Gaussian function is employed as the neighborhood function:

$$h_{wi}(t) = \alpha(t) \cdot \exp\left(-\frac{\left\| p_i - p_w \right\|^2}{2\sigma^2(t)} \right) \quad (2)$$

where p_i is the distance of vector position between the node i and winner node m_w, $\alpha(t)$ is some monotonic decreasing function with t, $\sigma(t)$ is also some monotonic decreasing function and defines the width of the kernel. In this study, $\alpha(t)$ and $\sigma(t)$ are given by

$$\begin{cases} \alpha(t) = \alpha(0)\dfrac{T-t}{T} \\ \sigma(t+1) = 1 + \left(\sigma(t) - 1\right)\dfrac{T-t}{T} \end{cases} \quad (3)$$

The final step is classification of input vectors onto the two-dimentional map. Every input vector is compared with all the reference vectors, and each of the input vectors is classified in the node to which the best much reference vector belongs.

3.2. Quantization Error (QE)

SOM composes nodes and reference vectors on two-dimentional map, assigning every input vectors to the node in which most similar reference vector exists. In this study, classification accuracies for each of the nodes are evaluated by QE, which for the ith node on the map is given by

$$QE_i = \frac{1}{m}\sum_{k=1}^{m}\sqrt{\frac{1}{d}\sum_{j=1}^{d}\left(x_j - r_j\right)^2} \quad (4)$$

where subscript i indicates the ith node on the map, m is number of input vectors assigned into the node i, d is the dimension of input vector. Low value of QE in the ith node indicates that input vectors in the ith node shows good similarities for their reference vector.

3.3. Non-Exceedance probability

The non-exceedance probability time series of climate indices are computed using the following plotting position formula.

$$F\left[x(i)\right] = \frac{i - \alpha}{N + 1 - 2\alpha} \quad (5)$$

where N is the number of samples, i is the ordered rank of a sample value. In this study, the rank is given from the smallest to the largest to obtain non-exceedance probabilities. The parameter α is set as 0.

4. RESULTS & DISCUSSION

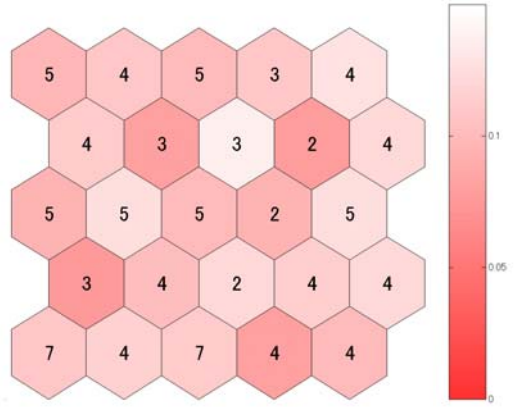

Figure 2. The map obtained by applying SOM for the 102 inputs. The number written in each node indicates the number of data classified in the node. QE of each node is shown in red colour.

4.1. Classification of annual averaged climate indices

In this section, we classify the four kinds of climate indices, which are SOI, PDOI, NPI and DMI, in order to identify the climate patterns represented by them.

As the first step, we compute annual averages for each of the four indices and then transform each of the time series into non-exceedance probability time series. As a result, we obtain 102 inputs, each of which shows climate pattern of the nth year (see below).

$$input\ 1 = (SOI_{1901}, PDOI_{1901}, NPI_{1901}, DMI_{1901})$$
$$input\ 2 = (SOI_{1902}, PDOI_{1902}, NPI_{1902}, DMI_{1902})$$
$$\vdots$$
$$input\ n = (SOI_{1900+n}, PDOI_{1900+n}, NPI_{1900+n}, DMI_{1900+n})$$
$$\vdots$$
$$input\ 102 = (SOI_{2002}, PDOI_{2002}, NPI_{2002}, DMI_{2002})$$

Subscript on each indices shows the year. Notice that each of the indices is transformed into non-exceedance probability; all components of input vectors are in the range between 0 and 1. Figure 2 illustrates the result of applying SOM for these 102 inputs. The SOM classifies the 102 years of climate patterns represented by the four indices onto the 25 nodes, as shown in the figure. For the rest of this paper, the map shown in Figure 2 will be referred to as CI-map (i.e. Climate Indices-map). Furthermore, sequence of numbers, which starts from top left of CI-map and end in bottom right on the map, is given for each node. For instance, the node number 1 is given for the node on the top left, 5 for the top right, 21 for the left bottom and node

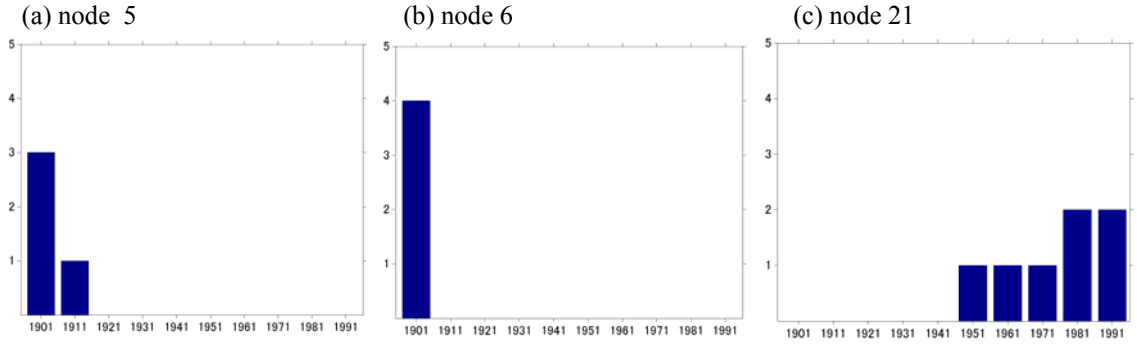

Figure 3. Histograms which shows the years of data classified in each node. Histogram (a) is drawn for the node 5, (b) is for the node 6 and (c) is for the node 21. Horizontal axis shows each of 10 years starts from 1901 and end in 2002. For instance, 1901 in the horizontal axis means the 10 years from 1901 to 1910 and vertical axis shows how many data in the node are in the 10 years.

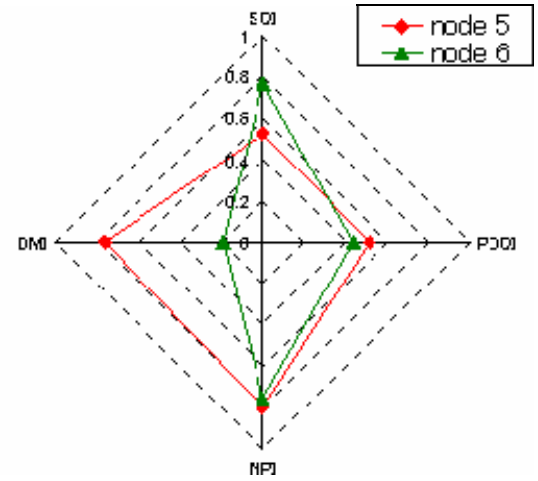

Figure 4. Radar chart of reference vector for the node 5 (drawn in red) and for the node 6 (drawn in green). Each of the 4 axes shows non-exceedance probalilities of SOI (top), PDOI (right), NPI (bottom) and DMI (left)

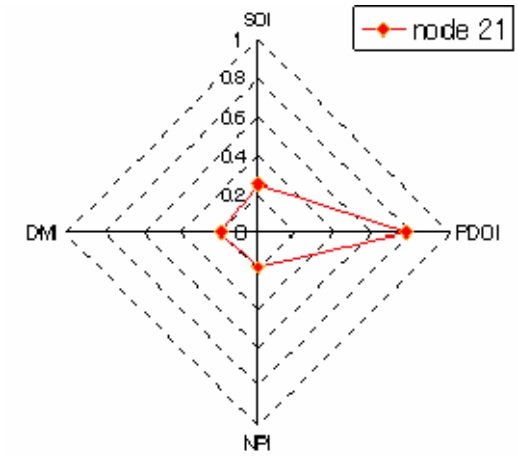

Figure 5. Radar chart of reference vector in node 21 (axes are the same as figure 5)

number 25 for the node on the bottom right on the CI-map.

As the next step, we examine the shift of climate patterns during the 102 years considered. Figure 3 (a) and (b) shows that climate patterns in node 5 and 6 occurred before 1921 and these patterns have not occurred since 1921, suggesting possible changing of frequency of the appearance in the climate Figure 3(c) indicates that climate pattern in the node 21 has appeared only since the 1950s.

Figure 4 is a radar chart of the representative pattern (i.e. reference vector) in the node 5 and 6. Both of the patterns show neutral value for PDOI and high value for NPI, while the pattern in the node 6 shows high value for SOI and low value for DMI, indicating the occurrence of La Niña in the Pacific Ocean and negative mode of dipole mode phenomenon in the Indian Ocean. Figure 3(c) shows the representative pattern in node 21, which has appeared since around the 1960s. In particular, this pattern has increasingly occurred since the 1980s. Climate pattern in Figure 5 shows strong negative modes (approximately 0.2 in non-exceedance probability) for SOI, NPI and DMI in contrast with the strong positive mode of PDOI.

4.2. Relationships between climate pattern and rainfall and temperature in Fukuoka

In this section, we investigate the relationships between the identified climate patterns and rainfall and temperature in Fukuoka, Japan. For each node of the CI-map, we create histograms, each of which shows the distribution of annual rainfall (or annual averaged temperature) in the same year when the climate pattern in the node occurs. We also draw histograms of annual rainfall and temperature for the next year against the

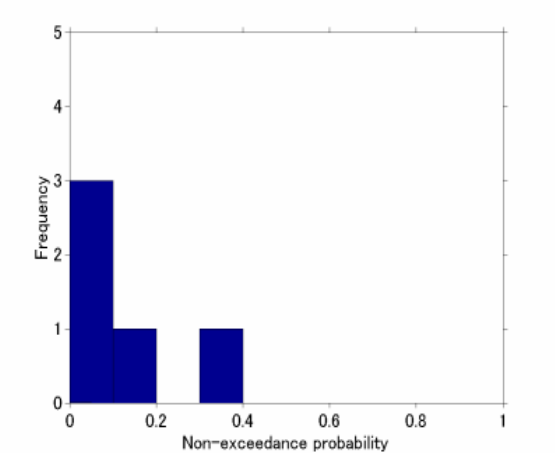

Figure 6. Histogram of non-exceedance probabilities in Fukuoka for the next year of the appearance of pattern in the node 1 Horizontal axis shows the temperature in Fukuoka transformed into the non-exceedance probabilities and vertical axis shows frequency.

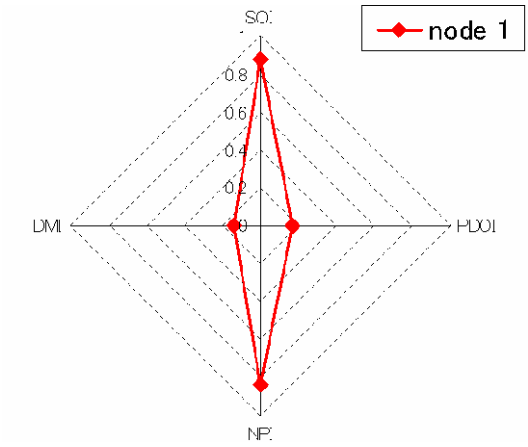

Figure 7. Radar chart of reference vector in node 1 (axes are the same as figure 5)

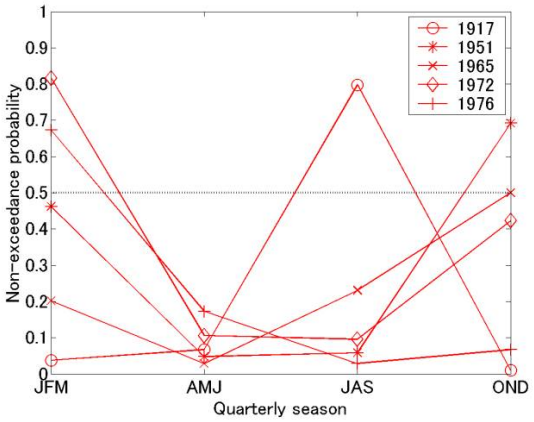

Figure 8. Linear plot of three months averaged (JFM; January, February, March, AMJ; April, May, June, JAS; June, August, September, OND; October, November, December) non-exceedance probabilities in Fukuoka for the next year of the appearance of climate pattern in node 1. Horizontal axis shows the three month averaged season (i.e. JFM, AMJ, JAS and OND) and vertical axis shows corresponding non-exceedance probabilities.

appearance of the climate pattern in each node, in order to examine possible time lags between the presence of a climate pattern and the response of weather in regional scale.

As a result, remarkable tendency between climate pattern in the node 1 and unusual low temperature of Fukuoka in the next year is detected (Figure 6). Notice that the 1 year lagged annual mean temperature is transformed into non-exceedance probability. Figure 7 gives a radar chart of the representative climate pattern (i.e. reference vector) in node 1. Considerable feature on Figure 7 is the remarkable high values of SOI and NPI, while extremely low values for PDOI and DMI. The climate patterns in node 1 occurred in the years 1916, 1950, 1964, 1971 and 1975 (during the past 102 years), and Figure 6 indicates when a year shows climate pattern in node 1, the annual averaged temperature in Fukuoka for the next year is lower than that in normal years.

As a next step, we divide each year into quarter terms which are JFM (January, February and March), AMJ (April, May and June), JAS (July, August and September) and OND (October, November and December), in order to evaluate the impacts of the climate pattern in the node 1 on variation of temperature in quarterly time scale. Quarterly variation of temperature in the next year for the appearance of climate pattern in node 1 is shown in Figure 8. As can be seen, when climate pattern in a year is in node 1, most of quarterly term temperature in the next year tends to show lower values than usual. In particular, quarterly terms of AMJ and JAS manifest remarkably low temperatures.

5. CONCLUSION

This study conducted classification of climate indices on yearly basis and examined the response of rainfall and temperature in Fukuoka for the identified climate patterns.

The classification of climate indices identified climate patterns which appeared in the first two decades of twentieth century and also detected the patterns which have been observed since the 1960s.

Investigation of the relationships between the identified climate pattern and rainfall and temperature in Fukuoka revealed that when La Niña phenomenon happened, PDO was in strong negative phase, the development of Aleutian low was weak and dipole mode in the Indian Ocean was in strong negative mode, AMJ and JAS temperature of Fukuoka in the next year tended to become extremely low.

6. REFERENCES

Allan, R.J., N. Nicholls, P.D. Jones and I.J. Butterworth (1991), further extension of the Tahiti-Darwin SOI, Early ENSO events and Darwin pressure, *Journal of Climate*, 4 743-749

Beniston, M., M. Rebetez, F. Giorgi and M.R. Marinucci (1994), An analysis of regional climate change in Switzerland, *Theoretical and Applied Climatology*, 49(3), 135-159

Japanese Study Group for Climate Impact & Application (1999), *El Niño & Global Environment*, Seizando, Japan (in Japanese).

Jin, Y.H., A. Kawamura, K. Jinno and Y. Iseri, (2003), On the long-term variability of Southern Oscillation Index, *Proc. of 2003 Korea Water Resources Association,* 151-158.

Kawamura, A., A.I. McKerchar, R.H. Spigel, and K. Jinno (1998), Chaotic characteristics of the Southern Oscillation Index time series, *Journal of Hydrology*, 204, 168-181.

Kawamura, A., S. Eguchi, K. Jinno and A. McKerchar (2002), Statistical characteristics of Southern Oscillation Index and its barometric pressure data. *Journal of Hydroscience and Hydraulic Engineering*, 20(2), 41-49.

Kohonen, T. (1998), The self-organizing map, *Neurcomputing*, 21, 1-6

Mantua, N.J., S.R. Hare, Y. Zhang, J.M. Wallace and R.C. Francis (1997), A Pacific interdecadal climate oscillation with impacts on salmon production, *Bulletin of the American Meteorological Society,* 78, 1069-1079

Qian W. And Y. Zhu (2001), Climate change in China from 1880 to 1998 and its impact on the environmental condition, *Climate Change*, 50(4), 419-444

Ropelewski C.F. and M.S. Halpert (1987), Global and regional scale precipitation Patterns associated with the El Nino/Southern Oscillation, *Monthly Weather Review*, 115(8), 1606-1626

Ropelewski, C.F. and P.D. Jones (1987), An extension of the Tahiti-Darwin Southern Oscillation index, *Monthly Weather Review*, 115, 2161-2165.

Saji, N.H., B.N. Goswami, P.N. Vinayachandran, and T. Yamagata (1999), A dipole mode in the tropical Indian Ocean, *nature*, 401 , 360-363

Trenberth, K.E. and J.W. Hurrel (1994), Decadal atmosphere-ocean variations in the Pacific. *Climate Dynamics*, 9, 303-319

Zhang, Y., J.M. Wallace and D.S. Battisi (1997). ENSO-like interdecadal variability 1900-1993, *Journal of Climate*, 10, 1004-1020